ceramics

MDPI

Article

Process for the Preparation of Artificial Analog of Sanbornite–Glass Composites

Jacob Hormadaly [1,*], Mariana Dov [1], Lonia Friedlander [2] and Natalia Pears [1]

[1] Department of Chemistry, Ben-Gurion University, Hashalom St. #1, P.O. Box 653, Beer-Sheva 84105, Israel; dovma@bgu.ac.il (M.D.); pears@bgu.ac.il (N.P.)
[2] Ilse Katz Institute for Nanoscale Science and Technology, The Ben-Gurion University of the Negev, Beer-Sheva 84105, Israel; friedlal@bgu.ac.il
* Correspondence: hormadj@bgu.ac.il

Abstract: Barium silicates have been investigated as high-expansion components of solid oxide fuel cells (SOFCs) and, therefore, their synthesis and expansion have been the subject of intensive research in recent years. In this article, we briefly present a new process to make glass–crystalline composites, as well as two novel findings related to a synthesis route of sanbornite ($BaSi_2O_5$) and the fast in situ formation of a high-expansion sanbornite composite from a Pyrex-type glass powder. The low-temperature synthesis, composition, and expansion of one type of novel glass composite are described. The composites are made by the reaction of $BaCO_3$ and Pyrex-type powders at 850–950 °C for a short time of one hour. The composites are well sintered and hard, and their linear coefficient of thermal expansion is about 12.3×10^{-6} C^{-1}. The crystalline-phase formation, dilatometer measurements, SEM data, and possible applications of the composites are presented and discussed.

Keywords: glass-composites; pyrex glass; sanbornite; synthesis

Citation: Hormadaly, J.; Dov, M.; Friedlander, L.; Pears, N. Process for the Preparation of Artificial Analog of Sanbornite–Glass Composites. *Ceramics* **2024**, *7*, 1994–2005. https://doi.org/10.3390/ceramics7040124

Academic Editor: Enrico Bernardo

Received: 14 October 2024
Revised: 24 November 2024
Accepted: 5 December 2024
Published: 18 December 2024

1. Introduction

Glass–ceramics [1–9] have been prepared by two methods: (1) the controlled crystallization of a base glass; and (2) the sintering and crystallization of a powdered glass. An updated definition of and new methods to generate glass–ceramics [6] have broadened the scope of this field. Here, we present only one aspect of a new process to synthesize glass–crystalline composites (a mixture of glass/es and crystalline phase/s) by the reaction of crystalline-phase $BaCO_3$ with a vitreous-phase Pyrex-type glass powder. The product of the reaction is crystalline-phase sanbornite ($BaSi_2O_5$) and a residual glass. The Pyrex-type glass powder serves as an active SiO_2 source. It crystallizes by itself upon heating but does not crystallize when heated with $BaCO_3$; it reacts with barium carbonate to form crystalline-phase sanbornite and a residual glass. This new process differs from the glass–ceramic process in the following two aspects: (1) the glass powder (Pyrex powder) does not crystallize in the process; (2) the composition of the crystalline phase formed is predetermined by the selection of the crystalline phase/s to react with the Pyrex powder. The new process is not reactive sintering because the Pyrex-type glass powder reacts with the barium carbonate and is consumed during the heat treatment process. In this article, we address one reaction only: that of Pyrex-type barium carbonate to form a sanbornite–residual glass composite.

The new process is detailed by Hormadaly [10] for a variety of crystalline phases synthesized with Pyrex-type glass powder. Reference [10] details the synthesis of seven compounds which are the artificial analogues of seven minerals (listed below) by the use of crystalline phases selected from alkaline earth carbonates ($CaCO_3$, $SrCO_3$, and $BaCO_3$), transition metal oxides (TiO_2, CuO), post-transition oxide (SnO_2), and Pyrex-type glass powder: (1) Sanbornite ($BaSi_2O_5$), the subject of this article; (2) Colinowensite ($BaCuSi_2O_6$); (3) Cuprorivaite ($CaCuSi_4O_{10}$); (4) Wesselsite ($SrCuSi_4O_{10}$); (5) Effenbergerite ($BaCuSi_4O_{10}$); (6) Fresnoite ($Ba_2TiSi_2O_8$); and (7) Pabstite (Ba (Ti,Sn)Si_3O_9).

Glass compositions have been used to seal, bond, and encapsulate electrical and electronic components because of their insulating properties, expansion, chemical durability, and viscosity. Glass compositions also serve as important ingredients for a variety of thick film pastes and electronic components such as low-temperature cofired ceramics (LTCCs).

The coefficient of thermal expansion (CTE) is a prime property in sealing, bonding, and the encapsulation of materials (ceramics and metals) with glasses; the CTE of the materials has to almost match (with a value of $\pm 1 \times 10^{-6}$ °C^{-1}) the CTE of the glass (or the glass-based material used for sealing) to prevent excessive stresses, cracking, and delamination. For sealing materials, there are special glass compositions available from glass manufacturers. For operations at a low temperature (for example, an overglaze for electronic circuits on 96% alumina substrates with sealing at low temperatures < 500 °C), a single glass composition is not sufficient. Sealing and encapsulation at low temperatures require low-softening-temperature glasses, which usually have a high CTE and are mainly lead- and bismuth-based glass compositions [11–13]. These low-softening-temperature glasses are modified by the inclusion of low-CTE fillers, such as vitreous silica, to lower the CTE. Sealing and encapsulation at a low temperature require a very short time at the peak temperature (usually 1–2 min). The sealing and bonding of materials used in solid-oxide fuel cells (SOFCs) require high-expansion glass-based materials, which have to withstand a high operating temperature and cycling [14]; therefore, the glass has to have a high glass transition temperature (T_g). These high-CTE glass-based materials are selected from high-T_g glass compositions and high-CTE fillers such as polycrystalline barium silicates. Both the low- and high-temperature sealings described above necessitate fillers that may be considered inert. For low-temperature sealing, because of the very short duration at the peak temperature, the interaction of the glass with the filler is minimal. For the high-temperature sealing of SOFCs, the interaction of the high-T_g glass (which has a high viscosity) with the high-expansion filler is also minimal. Another way to increase the CTE of a glass composite is by using crystallizable glass, which crystallizes the high-CTE crystalline phase after sealing and thermal treatment. Materials such as high-expansion LTCC also necessitate high-CTE glass-based materials [15].

Kerstan et al. [16] studied the expansion of various barium silicates by dilatometry and high-temperature X-ray diffraction and discussed the application of glass containing barium for SOFCs. Gorelova et al. [17] reported the results of high-temperature X-ray diffraction studies of barium silicates and discussed their crystal chemistry and anisotropy of thermal expansion. Applications of barium silicates to SOFCs and luminescence were also discussed. Reis et al. [18] detailed sanbornite-based glass–ceramic sealing for high-temperature applications.

Interactions between barium-containing materials (glass, glass–ceramics, and crystalline barium silicates) and Cr-bearing stainless steel interconnects (components of SOFCs) are well studied and documented [19–22]. The glass–crystalline composites, the subject of this paper, may react in a similar fashion to other barium-containing materials and form a high-TCE $BaCrO_4$ phase and other volatile Cr-species, such as CrO_3 and $CrO_2(OH)_2$. Therefore, the application of a buffer layer of crystallizable glass sealant free of barium and strontium should be considered before the application of glass–sanbornite composites.

Based on our recent findings [10,23] of the high reactivity of $BaCO_3$ with vitreous phases and especially Pyrex-type glass, we wish to present here a new process to make glass–crystalline composites and a novel glass composite based on the reaction of $BaCO_3$ and Pyrex-type glass powders. This paper presents the expansion data, composition, and thermal processing of the novel glass composite based on $BaCO_3$ and Pyrex-type glass powders. The high-expansion glass composite (12.4×10^{-6} °C^{-1}) is formed during the heating cycle. This novel approach is also a moderate-temperature synthesis method for barium silicate (sanbornite) glass composites. Future publications will deal with the reaction of barium carbonate with Pyrex-type glass powder as a function of temperature and the synthesis of complex silicate–glass composites (from Pyrex-type glass powders and alkaline earth carbonates, transition metal oxides, and post-transition metal oxides) to demonstrate that the new method is not limited to one type of glass composite.

2. Experimental Section

Waste pieces of Pyrex-type glass (Borosilicate glasses under the trademark Pyrex®, were introduced in 1915 by the Corning Glass Works company, Corning, NY, USA). Similar compositions are made by other companies and, for the purposes of this paper, are all referred to as Pyrex-type glass. The borosilicate glass called "DURAN" from Schott Glaswerke of Mainz, Germany, type number 8330, has the following properties: glass transition temperature (T_g) of 530 °C, softening temperature (T_s) (viscosity η of the glass is $10^{7.6}$ dPa·s) of 815 °C, and working temperature (η = 10^4 dPa·s) of 1270 °C (Kiefer et al.) [24]. Composition of Pyrex-type glass (Corning 7740 and Kimble (Owens-Illinois, Perrysburg, OH, USA) KG-33) is given by Bansal and Doremus [25,26] in wt.% as follows: SiO_2—81; B_2O_3—13; Na_2O—4; and Al_2O_3—2). The glass was cleaned with water, then rinsed with ethanol and manually broken into a powder using stainless-steel mortar and pestle. Powder was sieved through 60-mesh screen (250 microns) and ball-milled with isopropanol for 24 h. The glass slip was sieved through 325-mesh screen. After evaporation of isopropanol, the powder was dried in oven at 100 °C.

The glass composite was prepared by grinding 3.0 g of ball-milled Pyrex-type glass powder, 3.99 g of $BaCO_3$, and 45 drops (about 2.2 mL) of 3% polyvinyl alcohol (PVA) solution in agate mortar. The molar ratio of $BaCO_3$ to SiO_2 (in the Pyrex-type glass powder) is 1:2; the content of SiO_2 in Pyrex glass is 81%. The bar was shaped from a slightly wet ground mixture of barium carbonate and glass powders. For Orton dilatometer, the sample size is 5 cm length, 4 to 6 mm width, and height of 4–6 mm. The (parallelepiped) bar was prepared by pressing slightly wet mixture of glass and barium carbonate between two (parallelepiped) bars of stainless steel to obtain a sample that could be used for the dilatometer. The bar was dried in oven at 100 °C then 150 °C for about 2 h, then the bar was placed on Pt foil and heated at 850–950 °C range for 1 h. The bars retained their shape during heating and were well sintered. Bars were cut by a saw to size (2 inches) and measured with an Orton dilatometer. Part of the sintered bar was ground in agate mortar and sent for X-ray analysis. The glass composite bar was cut and polished to result in parallel end faces. Linear coefficients of expansion in the temperature range of 25–850 °C, the glass transition temperature (T_g), and the dilatometric softening points (T_s) were measured with an Orton dilatometer, model 1000D (The Edward Orton Jr. Ceramic Foundation, Westerville, OH, USA), at heating rate of 3 °C/min. The measurement accuracy is ±10%.

Comparative study of the reactivity of $BaCO_3$ with crystalline SiO_2 (quartz), amorphous SiO_2, and SiO_2 of Pyrex-type glass was performed by reacting stoichiometric amounts of $BaCO_3$ and SiO_2 in Pt crucible. The weights of the starting materials, 2.0 g quartz (0.03328 moles), 3.2843 g $BaCO_3$ (0.01664 moles), 2.0 g amorphous silica (0.03328 moles), and 3.2843 g $BaCO_3$ (0.01664 moles), were monitored. After being heated at 850 °C for 4 h, the amorphous silica reacted completely; 4.5277 g was recovered out of an expected theoretical weight (assuming complete reaction of $BaCO_3$, i.e., complete loss of CO_2) of 4.5522 g. After being heated at 850 °C for 4 h, the quartz did not react completely; 5.1184 g was recovered out of an expected theoretical weight of 4.5522 g.

Pyrex-type glass reacts at lower temperatures and faster than amorphous and quartz silica. Here, we compared 2.4691 g Pyrex-type glass (Pyrex contains 81% silica, i.e., 2.4691 g of the Pyrex contains 2.0 g of silica) and 3.2843 g $BaCO_3$ (0.01664 moles), with molar ratio of BaO/SiO_2 of 1/2, which is the same ratio used for the above-mentioned samples. We also compared 2.0 g amorphous silica (0.03328 moles) and 13.137 g $BaCO_3$ (0.06657 moles), with a molar ratio of BaO/SiO_2 of 2/1. Theoretical expected weight loss (for complete loss of CO_2) is 0.5931 g for Pyrex–$BaCO_3$ and is 2.9291 g for amorphous silica–$BaCO_3$. Samples were heated 8 h at 650 °C, 700 °C, and 750 °C, and weights were recorded after each heating stage. Weight loss for Pyrex–$BaCO_3$ sample was 0.1439 g, 0.3396 g, and 0.625 g respectively, and the Pyrex–$BaCO_3$ sample reached the theoretical weight loss value after heating for 8 h at 650 °C, 700 °C, and 750 °C. Weight loss for amorphous–$BaCO_3$ sample after heating for 8 h at 650 °C, 700 °C, and 750 °C was 0.1169 g, 0.6242 g, and 1.6422 g, respectively. The amorphous–$BaCO_3$ sample after heating for 8 h at 650 °C, 700 °C, and 750 °C did not

react completely (it had expected theoretical weight loss of 2.9291 g for complete reaction). The reactivity of the different types of silica is as follows: SiO_2 (in Pyrex) > amorphous SiO_2 > quartz. Even though the surface area of amorphous silica (5 m^2/g) is higher than that of the Pyrex-type glass (2.12 m^2/g), the reactivity of the Pyrex-type glass is higher.

Phase formation due to reaction between $BaCO_3$ and Pyrex-type glass powder and heat treatment was measured by X-ray diffraction. An Empyrean powder diffractometer (Panalytical B.V., Almelo, The Netherlands) equipped with X'Celerator position-sensitive detector was used. Data were collected in the θ/2θ geometry using Cu Ka radiation (λ = 1.54178 Å) at 40 kV and 30 mA. Scans were run for ~15 min in a 2θ range of 10–60° in steps equal to ~0.03°.

Surface area was measured by the BET (Brunauer, Emmett, and Teller) method using Quantachrome Nova Touch LX3 (1900 Corporate Drive, Boynton Beach, FL, USA). Surface area of ball-milled Pyrex-type glass powder was 2.12 m^2/g.

$BaCO_3$ used was from BDH Chemicals LTD (Poole Dorset, BH 12 4NN, UK 1984 2. Buchner) (AnalaR, minimum assay 99.5%). Amorphous silica (99.8%) was obtained from Alfa Aeasar (26 Parkridge Road Ward Hill, MA, USA), with a surface area of 5 m^2/g (manufacturer data). Quartz (99.99%) was obtained from Cerac Inc. (Milwaukee, WI, USA)

3. Results and Discussion

The composition of the glass composite is based on our recent findings [23], in which we found that when $BaCO_3$ reacts with Pyrex-type glass powder, it forms $BaSi_2O_5$ (sanbornite) at temperatures higher than 800 °C. Therefore, we selected the starting materials' weights to provide a molar ratio of BaO/SiO_2 of one to two, using 3.0 g of Pyrex-type glass and 3.99 g of $BaCO_3$. Pyrex contains 81% SiO_2; thus, 3.0 g of glass has 0.81 × 3/60.086 moles SiO_2, and 3.99 g of $BaCO_3$ have 3.99/197.34 moles $BaCO_3$ (or BaO).

Figure 1 presents the XRD of the sintered bar (after 1 h at 900 °C; the sample code is JH-054-38). It shows only one crystalline phase, that of $BaSi_2O_5$ (sanbornite; PDF card # 01-071-1441). The residual glass contains all the ingredients of Pyrex with a reduced silica content (SiO_2, B_2O_3, Na_2O, K_2O, Al_2O_3, and traces of Fe_2O_3, MgO, and CaO) and perhaps some dissolved BaO.

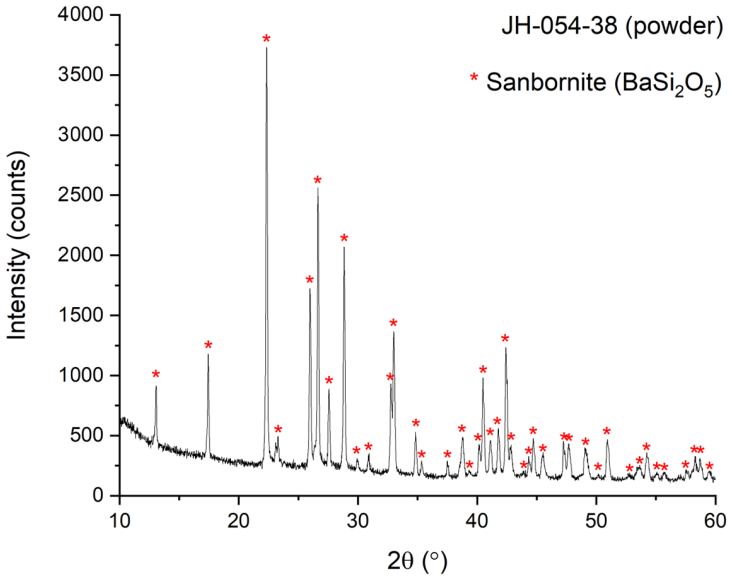

Figure 1. XRD of sintered bar at 900 °C for 1 h.

A dilatogram of JH-054-38 is given in Figure 2. Figure 2 shows that the percent linear change (PLC) is linear from room temperature to almost 500 °C (as also indicated by the constant value of the derivative of the coefficient of expansion (DCE)). The average linear coefficient of expansion in the 200–400 °C range is 12.7 × 10^{-6} $°C^{-1}$. The dilatometer

software selects the T_g (542 °C) and the dilatometer softening point T_s (821 °C) of the composite. The value of T_s is very high for the residual glass and will be referred to as the apparent dilatometer softening point. The measured apparent T_s is much higher than the T_s of Pyrex-type glass [24]. The difference between T_s and T_g ($T_s - T_g$) is very large and not typical for common glasses; a more detailed discussion of T_g and T_s will be given after the presentation of the dilatograms of bars made with the modified procedure. If we assume that all the silica in the Pyrex reacted to form sanbornite, then the sanbornite concentration is estimated as 90.66 wt.% and that of the residual glass is 9.34 wt.%. If we assume that only 75% of the silica in the Pyrex reacted to form sanbornite, we will obtain 67.7 wt.% sanbornite and 32.3 wt.% residual glass. If the concentration of the residual glass was high, the bars would deform. The bars did not deform at the 850–950 °C range, so the residual glass is estimated to be less that 30%. The residual glass probably has some dissolved BaO. For comparison, the T_g and T_s of Pyrex-type glass [25] are about 850 K and about 900 K, respectively (Figures 3 and 4 of reference [25]).

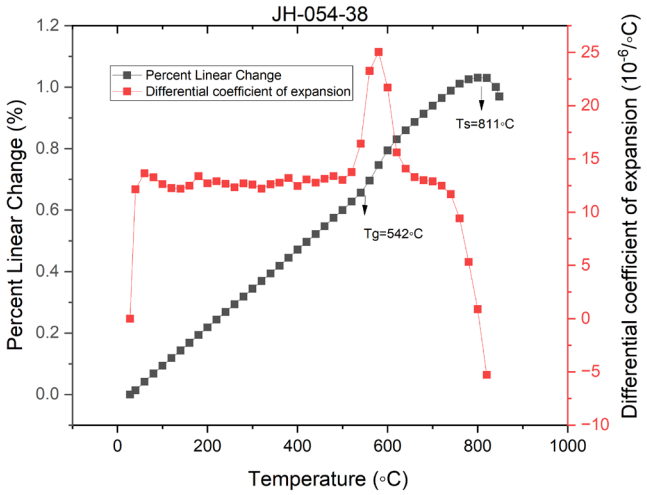

Figure 2. Dilatogram of a sintered bar for 1 h at 900 °C.

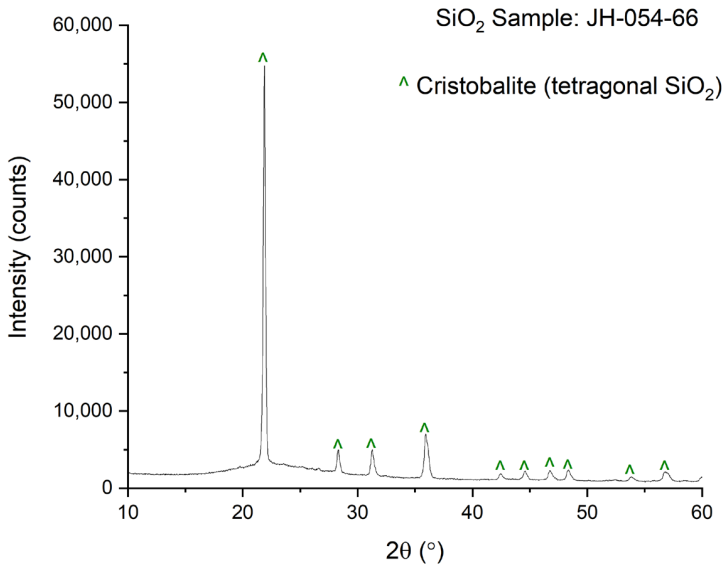

Figure 3. XRD of heat-treated (1 h at 900 °C) Pyrex-type glass.

The Pyrex-type glass was subjected to the same heat treatment used for code JH-054-38. The XRD of the heat-treated Pyrex-type powder (1 h at 900 °C; code JH-054-66) is given in Figure 3. Figure 3 shows that the powder of the Pyrex-type glass crystallizes after a 1 h heat treatment at 900 °C. All the lines in the crystalline phase can be assigned to α-

cristobalite. Figure 1 and the rest of the XRD figures (Figures 4–6) do not show the presence of cristobalite, even though the Pyrex by itself crystallizes when heated at 900 °C.

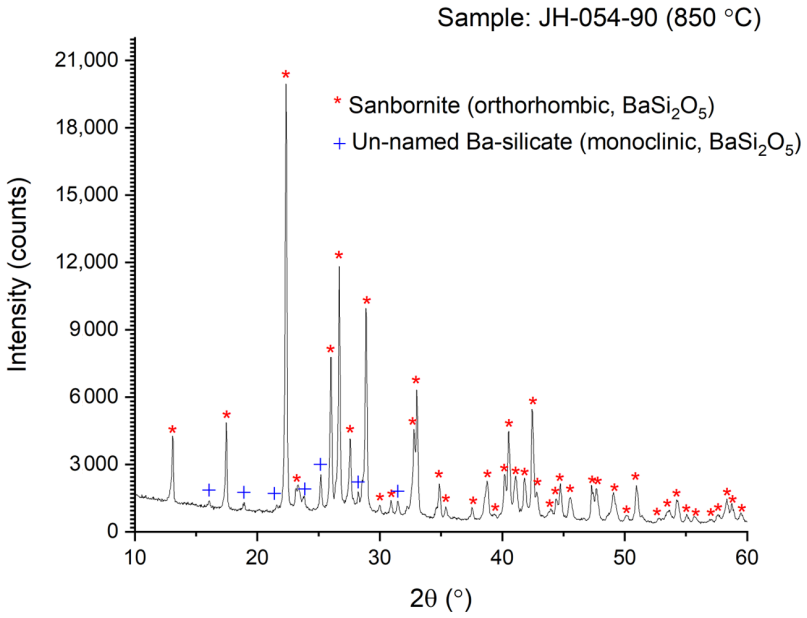

Figure 4. XRD of sintered bar at 850 °C for 1 h.

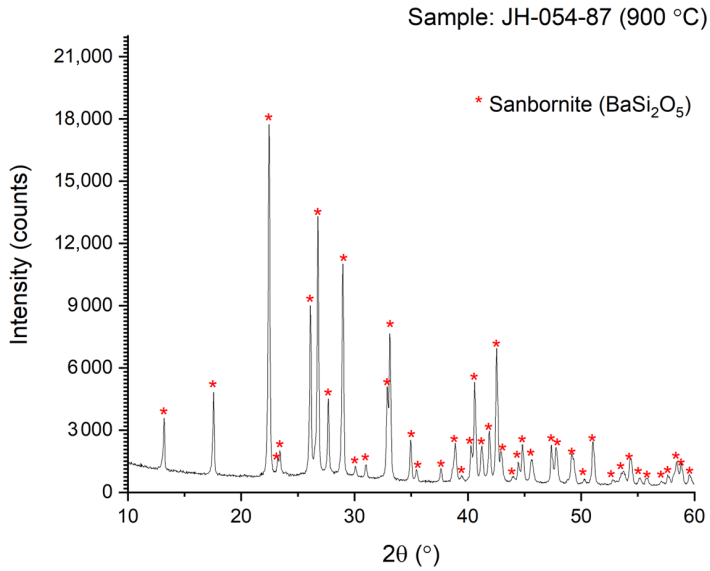

Figure 5. XRD of sintered bar at 900 °C for 1 h.

The procedure for the bar preparation was modified to include the following steps: extra grinding (to ensure the formation of homogeneous mixtures) of the $BaCO_3$ and Pyrex-type powders with isopropanol in an agate mortar, drying the mixture, grinding the mixture again with 45 drops of 3% PVA solution, shaping a bar, drying the bar on a hot plate, and then sintering. Three bars were prepared using the modified procedure. All three bars were prepared with the same materials and weights of sample code JH-054-38. The bars were sintered for 1 h at 850 °C, 900 °C, and 950 °C, and their codes are JH-054-90, JH-054-87, and JH-054-88, respectively. The bar sintered at 950 °C broke before the dilatometer measurements; the broken bar was used for the XRD only. A new bar identical to JH-054-88 was prepared, assigned the new code JH-054-92, and used for expansion measurements. The XRDs of sample codes JH-054-90, JH-054-87, and JH-054-88 are given in Figures 4–6, respectively.

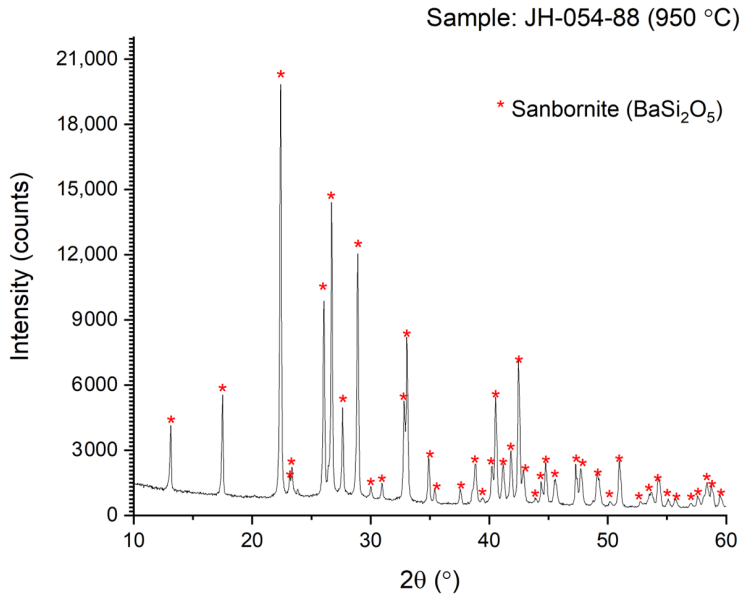

Figure 6. XRD of sintered bar at 950 °C for 1 h.

Figure 4 (the XRD of the sintered bar at 850 °C prepared by the modified procedure (with extra grinding)) shows the lines of sanbornite (PDF card # 01-071-1441; Pcmn (space group number 62)) as a major phase and faint lines of another phase of unnamed barium silicate (PDF card # 04-009-1825; Monoclinic $BaSi_2O_5$—C2/c (space group number 15)) as a minority phase. At 850 °C, the XRD shows lines of two phases of barium silicates, and at higher temperatures (Figures 5 and 6), only the sanbornite is stable (PDF card # 01-071-1441).

Figure 5 shows the XRD of the sintered bar at 900 °C prepared by the modified procedure (with extra grinding). The figure shows only lines of sanbornite.

Figure 6 presents the XRD of the sintered bar at 950 °C prepared by the modified procedure (with extra grinding). The figure shows only lines of sanbornite.

Figures 4–6 do not show the typical hump of the glassy phase, so it seems that the residual glass is below the detection limit of X-ray diffraction.

Samples codes JH-054-87 (with 900 °C sintering), JH-054-90 (with 850 °C sintering), and JH-054-92 (with 950 °C sintering), which are the sintered bars for the dilatometer measurements, were measured using an Orton dilatometer. Each sample was measured three times (after the first run, the sample was left in the dilatometer and run again (the codes were changed to JH-054-87A, JH-054-90A, and JH-054-92A), and after the second run, the sample was left in the dilatometer and run again for the third time (the codes were changed to JH-054-87B, JH-054-90B, and JH-054-92B). The data of run number 1 were discarded (in the first run, the bar may slightly move and can affect the measured TCE, while in the second and third runs, the bar is locked in the dilatometer and cannot shift) for the samples that were prepared by the modified procedure, except for sample code JH-054-38, which was measured only one time.

Figures 7–9 present the dilatograms of the third run of JH-054-90B (850 °C), JH-054-87B (900 °C), and JH-054-92B (950 °C), respectively. The dilatograms of JH-054-87B (900 °C), JH-054-90B (850 °C), and JH-054-92B (950 °C) are similar to the dilatogram of sample code JH-054-38. In all the dilatograms, the apparent dilatometer softening point is very high and well above 800 °C. The apparent dilatometer softening point increases with the sintering temperature: 809 °C (at 850 °C sintering), 832 °C (at 900 °C sintering), and 845 °C (at 950 °C sintering). The high apparent dilatometer softening point indicates the high viscosity of the composite and no distortion of the bars occurred, as was shown experimentally. All the bars retained their original shape after sintering (1 h) in the 850–950 °C range.

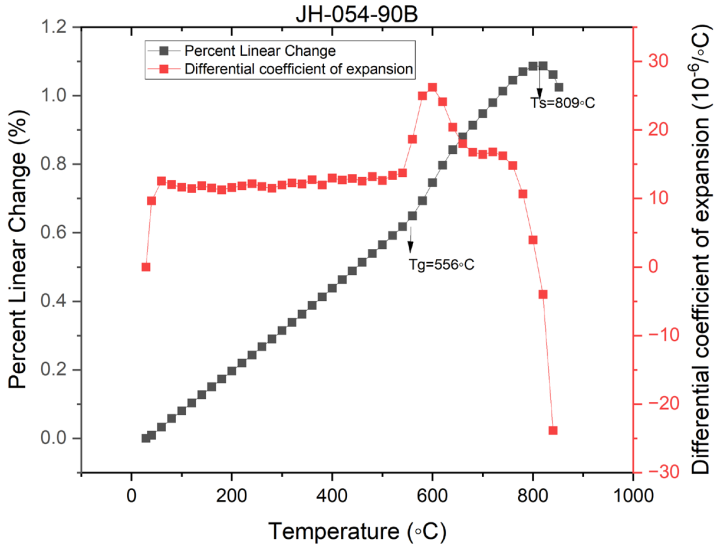

Figure 7. Dilatogram of third run of JH-054-90B (850 °C).

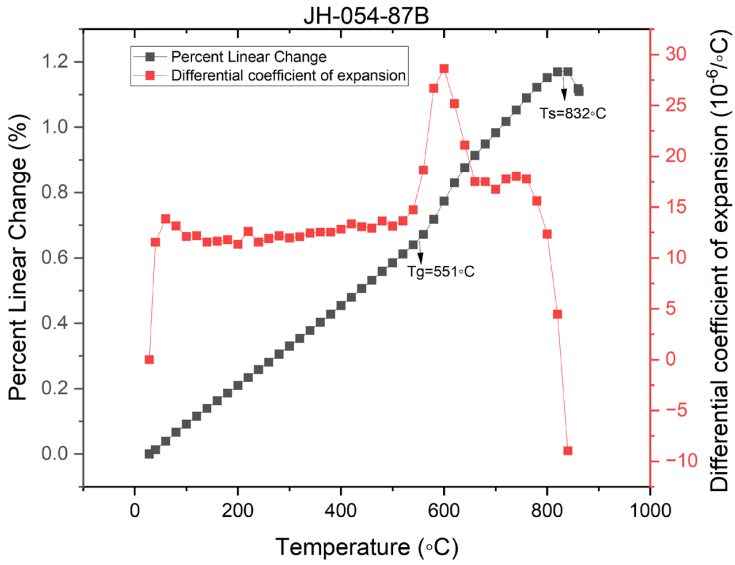

Figure 8. Dilatogram of third run of JH-054-87B (900 °C).

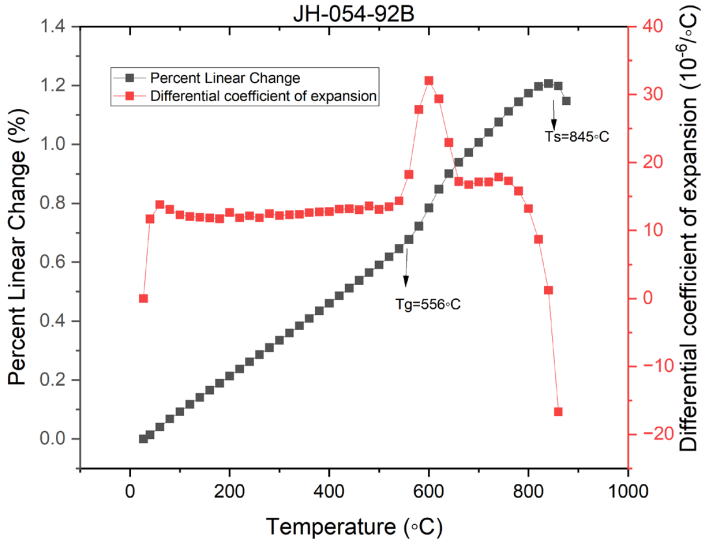

Figure 9. Dilatogram of third run of JH-054-92B (950 °C).

The T_g of the bars made by the modified procedure and sintered at 850 °C, 900 °C, and 950 °C (Figures 7–9) are 556 °C, 551 °C, and 556 °C, respectively. These values are the same (within the degree of experimental error) and may indicate the same composition for the residual glass.

Table 1 collects the dilatometer data for sample codes JH-054-38, JH-054-87, JH-054-88, and JH-054-92. Sample JH-054-38 was measured only one time (run number 1) and the other three samples were measured three times each (run numbers 1, 2, and 3). Run number 1 was discarded, and only the data for runs 2 and 3 were used to compare the samples. The average TCE (200–400 °C) of JH-054-87 (run numbers 2 and 3) is 12.3 × 10^{-6}/°C. The corresponding values for JH-054-90 and JH-054-92 are 11.95 × 10^{-6}/°C and 12.4 × 10^{-6}/°C, respectively. The TCE of JH-054-87 (900 °C sintering) and of JH-054-92 (950 °C sintering) are the same within the degree of experimental error. The corresponding TCE for JH-04-90 (850 °C sintering) is slightly lower: 11.95 × 10^{-6}/°C. All the samples in Table 1 have the same composition (sanbornite and residual glass); they differ in terms of the thermal treatment.

Table 1. Dilatometer data.

Sample Code	CTE (200–400 °C) × 10^6/°C	Heat Treatment	Run Number
JH-054-38	12.7	900 °C, 1 h	1
JH-054-87	10.6	900 °C, 1 h	1
JH-054-87A	12.4	900 °C, 1 h	2
JH-054-87B	12.2	900 °C, 1 h	3
JH-054-90	10.8	850 °C, 1 h	1
JH-054-90A	11.8	850 °C, 1 h	2
JH-054-90B	12.1	850 °C, 1 h	3
JH-054-92	12.7	950 °C, 1 h	1
JH-054-92A	12.4	950 °C, 1 h	2
JH-054-92B	12.4	950 °C, 1 h	3

The high-expansion crystalline-phase $BaSi_2O_5$ (sanbornite) is formed during a very short (1 h) heat treatment in the 850–950 °C range as a reaction product between $BaCO_3$ and Pyrex-type glass powder. Barium silicates are usually synthesized [13] at very high temperatures (1500–1550 °C) and require intermittent grinding. The data in Table 1 show that the window for processing is wide—at least 50 °C (samples JH-054-87B and JH-054-92B).

Three bars (codes JH-054-079A-C) were also prepared with the same materials and weights of sample code JH-054-38. The bars were sintered for 1 h at 850 °C, 900 °C, and 950 °C, respectively, and were used for SEM. The SEM pictures of sample codes JH-054-079A-C are given in Figures 10–12. Figure 10 shows the SEM of JH-054-079A (a sintered bar at 850 °C for 1 h), with many pores ranging in size from two to nine microns and a crystalline phase that is clearly shown by the white rods. Because of the large number of pores, the sintered sample might be porous with connected pores. Figure 11 presents the SEM of JH-054-079B (a sintered bar at 900 °C for 1 h). It shows fewer pores than JH-054-079A (a bar at 850 °C for 1 h), has pore sizes in the range of two to nine microns, and is more crystallized, shown by the white rods with some plate-like crystals. This sample might be porous, like a bar sintered at 850 °C for 1 h. Figure 12 presents the SEM of JH-054-079C (a sintered bar at 950 °C for 1 h). It shows a highly crystallized sample with a very small number of minute pores (with a size of about 1 micron), and the crystalline phase is shown by the white plates. JH-054-079C is probably a low-porosity sample. Figures 10–12 show that the microstructure can be controlled by thermal processing.

A comparison of the microstructures (SEM) with the dilatometer data shows that the effect of the microstructure on the linear coefficient of expansion of the composites is very small but the apparent dilatometer softening point (T_s) increases with the heat treatment temperature and the change in microstructure. The porous structure (JH-054-079A (a bar at 850 °C for 1 h)) has an apparent softening point (T_d) of 809 °C, and the denser structure (JH-054-079C (a sintered bar at 950 °C for 1 h)) has an apparent softening point (T_d) of 845 °C.

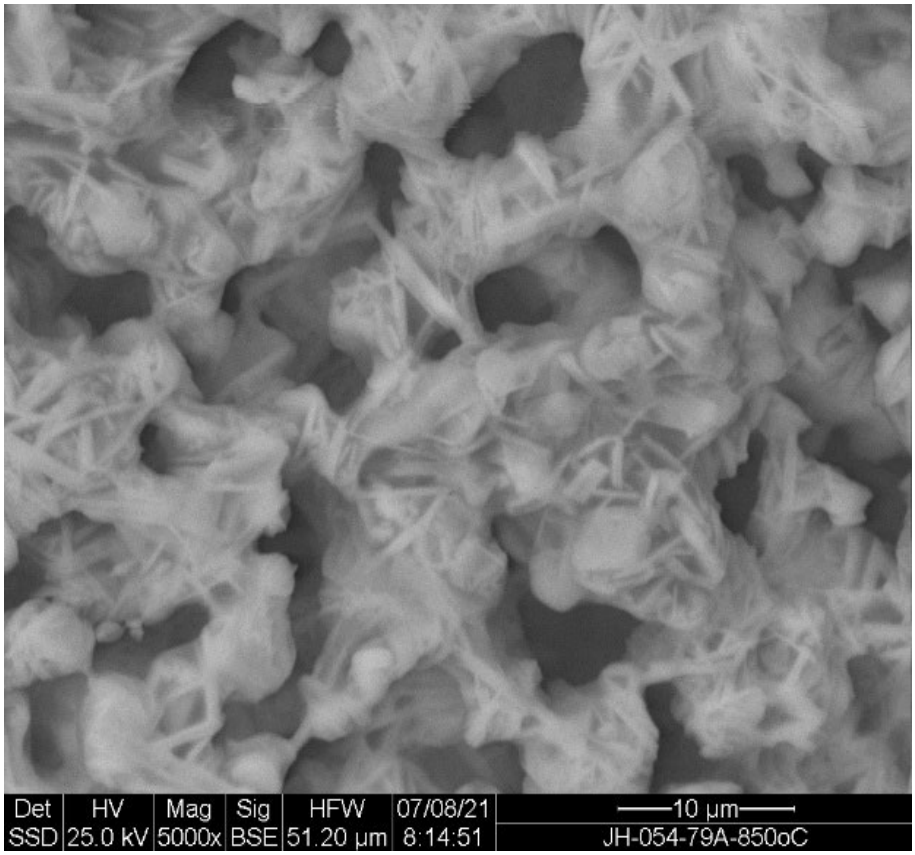

Figure 10. SEM of sample code JH-054-79A sintered bar at 850 °C for 1 h.

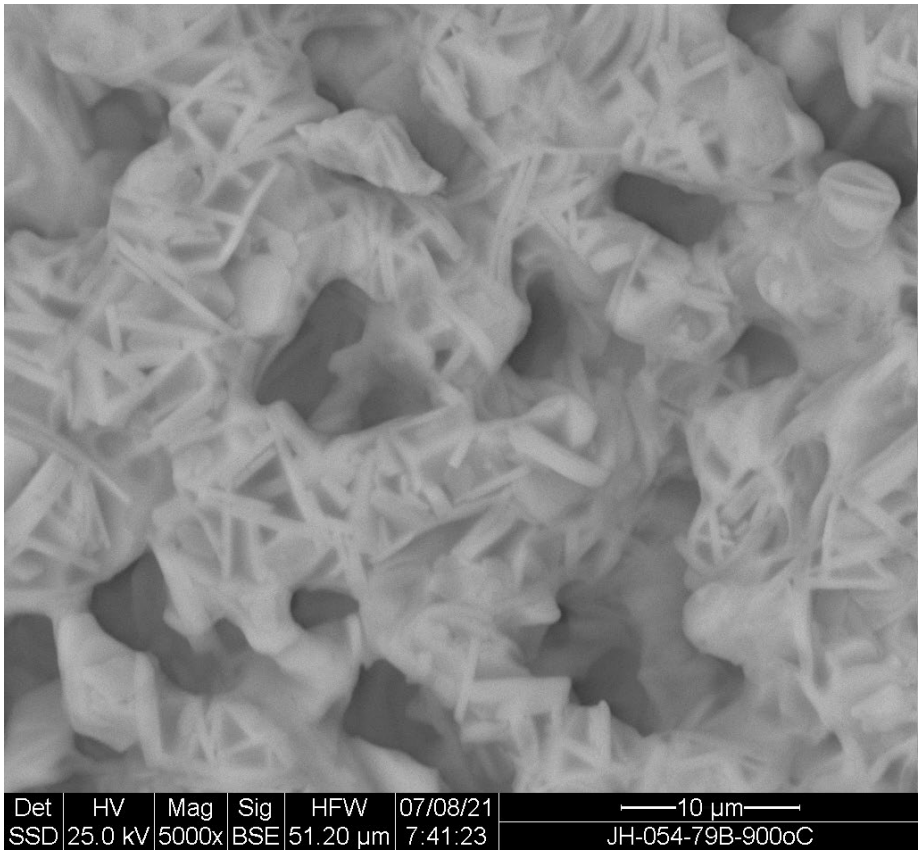

Figure 11. SEM of sample code JH-054-79B sintered bar at 900 °C for 1 h.

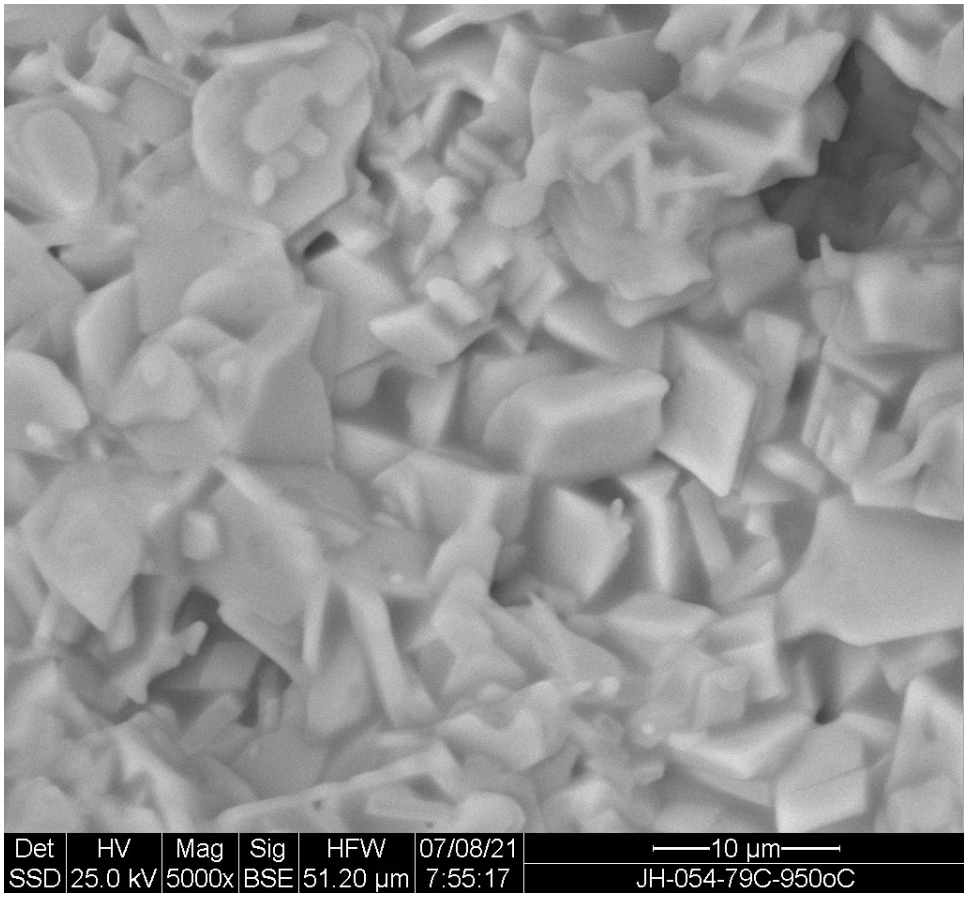

Figure 12. SEM of sample code JH-054-79C sintered bar at 950 °C for 1 h.

4. Summary and Conclusions

A new method to synthesize glass–crystalline materials was detailed for one material (a composite of sanbornite and residual glass derived from Pyrex-type glass). The type of crystalline phase ($BaSi_2O_5$) is not a function of the base glass composition but is predetermined by the selection of the crystalline reactant ($BaCO_3$).

The reactivity of barium carbonate with Pyrex-type glass was demonstrated for the preparation of high-expansion (12.4×10^{-6} °C^{-1}) $BaSi_2O_5$ (sanbornite) glass composites. High-expansion composites were synthesized as sintered bars at 850–950 °C, heating them for a short time of one hour. These novel high-expansion composites might be useful for SOFCs and LTCC.

Author Contributions: Validation, L.F.; Formal analysis, M.D., L.F. and N.P.; Investigation, J.H.; Data curation, M.D. and N.P.; Writing—original draft, J.H.; Supervision, J.H. All authors have read and agreed to the published version of the manuscript.

Funding: This research received no external funding.

Institutional Review Board Statement: Not applicable.

Informed Consent Statement: Not applicable.

Data Availability Statement: The original contributions presented in the study are included in the article; further inquiries can be directed to the corresponding author.

Conflicts of Interest: The authors declare no conflict of interest.

References

1. Stookey, S.D. Ceramic Body and Method of Making It. U.S. Patent 2,971,853, 1961.
2. Stookey, S.D. History of the development of pyroceram. *Res. Manag.* **1958**, *1*, 155–163. [CrossRef]
3. Stookey, S.D. Catalyzed crystallization of glass in theory and practice. *Ind. Eng. Chem.* **1959**, *51*, 805–808. [CrossRef]
4. McMillan, P.W. *Glass-Ceramics*; Academic Press: London, UK, 1964.
5. Höland, W.; Beall, G.H. *Glass Ceramic Technology*; The American Ceramic Society: Westerville, OH, USA, 2002.
6. Nakane, S. Recent research on Li_2O-Al_2O_3-SiO_2 glass-ceramics for expansion of applications. *J. Non Cryst. Solids X* **2022**, *16*, 100121. [CrossRef]
7. Zanotto, E.D. A bright future for glass-ceramics 89. *Am. Ceram. Soc. Bull.* **2010**, *89*, 19–27.
8. Nakane, S.; Kawamoto, K. Li2O-Al2O3-SiO2 Glass-Ceramics. U.S. Patent 9,126,859, 2015.
9. Deubener, J.; Allix, M.; Davis, M.J.; Duran, A.; Höche, T.; Honma, T.; Komatsu, T.; Krüger, S.; Mitra, I.; Müller, R.; et al. Updated definition of glass-ceramics. *J. Non Cryst. Solids* **2018**, *501*, 3–10. [CrossRef]
10. Hormadaly, J. Method of Manufacturing Porous Sintered Pyrex-Type Glass and Methods of Synthesizing Composites and Powders of Alkaline Earth Silicates. WO Patent 2022/101905, 19 May 2022.
11. Frieser, R.G. A review of solder glasses. *Act. Passiv. Electron. Compon.* **1975**, *2*, 163–199. [CrossRef]
12. Maeder, T. Review of Bi_2O_3 based glasses for electronics and related Applications. *Int. Mater. Rev.* **2013**, *58*, 3–40. [CrossRef]
13. Takamori, T. Solder glasses. In *Treatise on Materials Sciences and Technology*; Tomozawa, M., Doremus, R.H., Eds.; Academic Press: New York, NY, USA, 1979; Volume 17, p. 173.
14. Mahapatra, K.; Lu, K. Glass-based seals for solid oxide fuel and electrolyzer cells—A review. *Mater. Sci. Eng.* **2010**, *67*, 65–85. [CrossRef]
15. Eberstein, M.; Glitzky, C.; Gemeinert, M.; Rabe, T.; Schiller, W.A.; Modes, C. Design of LTCC with High Thermal Expansion. *Int. J. Appl. Ceram. Technol.* **2009**, *6*, 1–8. [CrossRef]
16. Kerstan, M.; Russel, C. Barium silicates as high thermal expansion seals for solid oxide fuel cells studied by high-temperature X-ray diffraction (HT-XRD). *J. Power Sources* **2011**, *196*, 7578–7584. [CrossRef]
17. Gorelova, L.A.; Bubnova, R.S.; Krivovichev, S.V.; Krzhizhanovskaya, M.G.; Filatov, S.K. Thermal expansion and structural complexity of Ba silicates with tetrahedrally coordinated Si atoms. *J. Solid State Chem.* **2016**, *235*, 76–84. [CrossRef]
18. Reis, S.T.; Schwartz, M.J.; Zandi, M.; Narendar, Y. Sanbornite-Based Glass-Ceramic Seal for High-Temperature Applications. U.S. Patent 10,658,684 B2, 19 May 2020.
19. Lahl, N.; Bahadur, D.; Singh, K.; Singheiser, L.; Hilpert, K. Chemical interactions between aluminosilicate base sealants and the components on the anode side of solid oxide fuel cell. *J. Electrochem. Soc.* **2002**, *149*, A607–A614. [CrossRef]
20. Yang, Z.; Meinhardt, K.D.; Stevenson, J.W. Chemical compatibility of barium-calcium-aluminosilicate-based sealing glasses with ferritic stainless steel in SOFCs. *J. Electrochem. Soc.* **2003**, *150*, A1095–A1101. [CrossRef]
21. Fregus, J.W. Sealants for solid oxide fuel cells. *J. Power Sources* **2008**, *184*, 238–244. [CrossRef]
22. Zhang, T.; Brow, R.K.; Fahrenholtz, W.G.; Reis, S.T. Chromate formation at the interface between a solid oxide fuel cell sealing glass and interconnect alloy. *J. Power Sources* **2012**, *205*, 301–306. [CrossRef]
23. Dov, M.; Pears, N.; Hormadaly, J. Synthesis of Pyrex–type porous glass made with calcium carbonate as pore forming material. *J. Non Cryst. Solids* **2021**, *564*, 120788. [CrossRef]
24. Kiefer, W.; Sura, M. Method of Manufacturing Porous Sintered Inorganic Bodies with Large Open Pore Volume. U.S. Patent 4,588,540, 13 May 1986.
25. Ota, K.; Botta, W.J.; Vaughan, G.; Yavari, A.R. Glass transition Tg, thermal expansion, and quenched-in free volume ΔVf in pyrex glass measured by time-resolved X-ray diffraction. *J. Alloys Compd.* **2005**, *388*, L1–L3. [CrossRef]
26. Bansal, N.P.; Doremus, R.H. *Handbook of Glass Properties*; Academic Press Inc.: Troy, NY, USA, 1986.